ACS OMEGA

http://pubs.acs.org/journal/acsodf

Article

Amphiphilic Rhenium-Oxo Corroles as a New Class of Sensitizers for Photodynamic Therapy

Rune F. Einrem, Abraham B. Alemayehu, Sergey M. Borisov,* Abhik Ghosh,* and Odrun A. Gederaas*

Cite This: *ACS Omega* 2020, 5, 10596−10601

Read Online

ACCESS | Metrics & More | Article Recommendations | Supporting Information

ABSTRACT: A set of rhenium(V)-oxo *meso*-triarylcorroles bearing ester and carboxylic acid functionalities were synthesized with a view to determining their potential for photodynamic therapy. Toward this end, we measured their near-IR phosphorescence and their ability to sensitize singlet oxygen formation. The two esters studied, $Re^{V}O$ 5,10,15-tris(*meta*-carbomethoxyphenyl)corrole and $Re^{V}O$ 5,10,15-tris(*para*-carbomethoxyphenyl)corrole, were found to exhibit phosphorescence quantum yields of around 1% and fairly long phosphorescence lifetimes of about 60 μs in toluene. The corresponding carboxylic acids, which were examined in ethanolic/aqueous media, in contrast, showed much lower phosphorescence quantum yields on the order of 0.01% and somewhat shorter phosphorescent lifetimes. The quantum yields for singlet oxygen formation, on the other hand, turned out to be equally high (0.72 ± 0.02) for the esters and corresponding carboxylic acids. For the two carboxylic acids, we also carried out photocytotoxicity measurements on rat bladder cancer cells (AY27) and human colon carcinoma cells (WiDr). Cell viability measurements (MTT assays) indicated 50% cell death (LD_{50}) for AY27 cells upon 5 min of blue light exposure with the meta carboxylic acid and upon 7 min of exposure with the para carboxylic acid; complete cell death resulted after 20 min for both compounds. The WiDr cells proved less sensitive, and LD_{50} values were reached after 8 and 12 min illumination with the meta and para carboxylic acids, respectively.

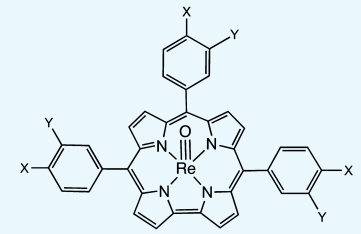

	X	Y
Re[T*p*CO_2CH_3PC](O)	CO_2CH_3	H
Re[T*m*CO_2CH_3PC](O)	H	CO_2CH_3
Re[*p*TCPC](O)	CO_2H	H
Re[*m*TCPC](O)	H	CO_2H

INTRODUCTION

Photodynamic therapy (PDT) relies on the combined action of a photosensitizer, light, and molecular oxygen to treat a variety of medical conditions, notably cancer and various skin conditions and increasingly also bacterial, viral, and fungal infections.[1,2] A common, but far from exclusive, mechanism involves photoexcitation of the sensitizer to a short-lived singlet excited state (S_1), intersystem crossing to a longer lived triplet state (T_1), and energy transfer to ground-state triplet oxygen ($^3\Sigma_g$), leading to highly reactive singlet oxygen ($^1\Delta_g$) as the primary cytotoxic species. From the very earliest days of PDT,[3] porphyrins have been a cornerstone of the method because of their preferential uptake and accumulation in tumors and other rapidly dividing cells, relative to normal tissues.[4−8] The recent efflorescence of the field of porphyrin analogues, particularly corroles,[9−12] now promises a plethora of new photosensitizers. Thus, gold triarylcorroles, which exhibit near-infrared (NIR) phosphorescence at room temperature, have been found to exhibit strong photocytotoxicity against cancer cells.[13−15] Other 5d metallocorroles, such as rhenium(V)-oxo[16] [but not rhenium(V)-imido[17]], osmium(VI)-nitrido,[18] iridium(III),[19] and platinum(IV)[20] corroles, have also been found to exhibit room-temperature NIR phosphorescence,[21−25] but their photocytotoxic behavior remains unexplored. Within this growing class of complexes, $Re^{V}O$ corroles are particularly attractive on account of easy accessibility and their impressive thermal, chemical, and photochemical stability. Presented herein, accordingly, are a set of $Re^{V}O$ *meso*-triarylcorroles bearing ester and carboxylic acid functionalities (Chart 1) and measurements of their NIR phosphorescence, sensitization of singlet oxygen formation,

Chart 1. Compounds Studied in This Work.

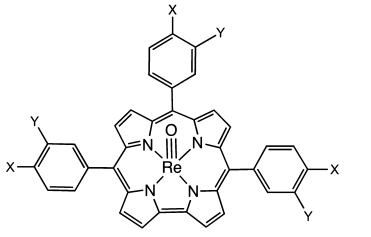

	X	Y
Re[T*p*CO_2CH_3PC](O)	CO_2CH_3	H
Re[T*m*CO_2CH_3PC](O)	H	CO_2CH_3
Re[*p*TCPC](O)	CO_2H	H
Re[*m*TCPC](O)	H	CO_2H

Received: March 11, 2020
Accepted: April 15, 2020
Published: April 27, 2020

https://dx.doi.org/10.1021/acsomega.0c01090
ACS Omega 2020, 5, 10596−10601

and photocytotoxicity vis-à-vis rat bladder cancer cells (AY27)[26−28] and human colon carcinoma cells (WiDr).[29] The results are promising and argue for more in-depth studies of the biomedical potential of $Re^{V}O$ corroles.

RESULTS AND DISCUSSION

Photophysical Properties. The compounds depicted in Chart 1 were synthesized via standard methods,[16] as described in the Experimental Section. The UV−vis spectra of the new complexes (Figures S1−S4) are also very similar to those of other $Re^{V}O$ corroles reported previously.[16] The new complexes were all found to exhibit NIR phosphorescence at room temperature, albeit with considerable differences between the lipophilic esters Re[T*m*CO_2CH_3PC](O) and Re[T*p*CO_2CH_3PC](O) (Figure 1A) and the corresponding

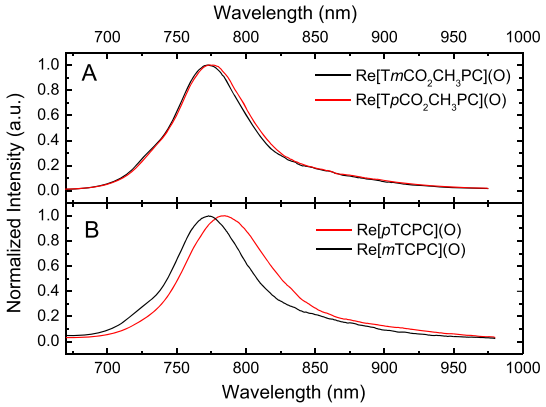

Figure 1. Phosphorescence spectra of $Re^{V}O$ corroles. (A) Carboxylic acid methyl esters (in anoxic toluene, λ_{ex} 440 nm, and 23 °C); (B) carboxylic acids (in anoxic EtOH with 3×10^{-3} M NaOH, λ_{ex} 432 nm, and 25 °C).

free acids Re[*m*TCPC](O) and Re[*p*TCPC](O) (Figure 1B). The two esters showed $\lambda_{max,em}$ values around 775 ± 2 nm, quantum yields of around 1% [relative to the Pt(II) tetraphenyltetrabenzoporpyhrin (Pt[TPTBP])],[30] and phosphorescence lifetimes of about 60 μs (Table 1). The phosphorescence decay was found to be monoexponential (Figures S5 and S6).

The $Re^{V}O$ corrole free acids exhibit much weaker NIR phosphorescence, with quantum yields below 0.1%, more than an order of magnitude below those measured for analogous lipophilic $Re^{V}O$ corroles. However, because ethanol was used as the solvent in these measurements to ensure solubility of the more hydrophilic free acids, efficient radiation-less deactivation via O−H vibrations might be an important factor behind the low quantum yields.[31,32] Addition of small amounts of NaOH to the ethanolic solutions led to slight enhancements of the quantum yields as well as to small hypsochromic shifts (∼6 nm) of the emission maxima (Table 2). The enhancement of

Table 2. Photophysical Properties of Amphiphilic ReO Corroles at 25 °C in Anoxic solutions

complex	Solvent	$\lambda_{max,em}$ (nm)	ϕ (%)	τ (μs)
Re[*p*TCPC](O)	EtOH	783	∼0.03	38 (91%), 1.2 (9%)
Re[*p*TCPC](O)	EtOH + 3×10^{-3} M NaOH	777	∼0.05	27 (73%), 1.0 (27%)
Re[*m*TCPC](O)	EtOH	773	∼0.01	5.9 (44%), 1.3 (56%)
Re[*m*TCPC](O)	EtOH + 3×10^{-3} M NaOH	766	∼0.02	13 (23%), 1.7 (77%)

the phosphorescence quantum yields may be a result of deaggregation of the dyes upon deprotonation of the COOH groups. The phosphorescence decay times are not monoexponential (Figures S7−S10), which might reflect the existence of several species (monomers/dimers). Interestingly, in the basic solutions, the contribution of the shorter- lifetime component appears to increase. The dyes are also soluble in water at basic pH values, but the phosphorescence turned out to be even weaker, with quantum yields below 0.001%. Evidently, radiationless deactivation of the excited states is even stronger than in ethanol. The overall conclusion from the data is that Re[*m*TCPC](O) is a weaker emitter than Re[*p*TCPC](O), with the former exhibiting quantum yields about half that of the latter, a finding consistent with the shorter phosphorescence decay times of the former complex.

Sensitization of Singlet Oxygen Formation. The efficiency of singlet oxygen formation was evaluated with an assay using 9,10-dimethylanthracene (DMA) as a singlet oxygen acceptor[33] and methylene blue as a sensitizer with a known quantum yield for singlet oxygen formation (Φ_Δ = 0.48).[21] Figure 2 shows the kinetics of decomposition of DMA

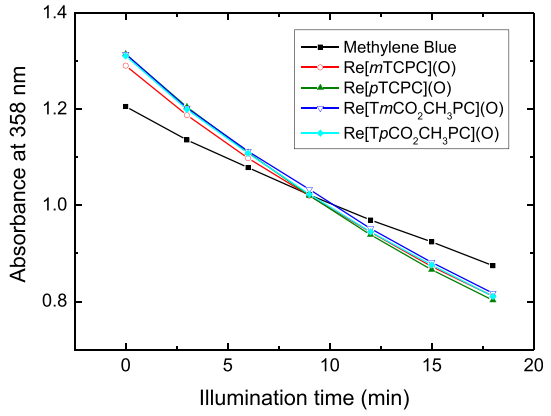

Figure 2. Kinetics of degradation of DMA (0.2 mM) of an air-saturated solution in EtOH/THF (9:1 v/v) upon irradiation with 595 ± 5 nm light in the presence of a sensitizer. Note that the absorbance at 358 nm reflects the contribution of the sensitizer and of the acceptor.

Table 1. Photophysical Properties of Lipophilic $Re^{V}O$ Corroles in Anoxic Toluene at 23 °C: Maxima of the Absorption and Emission Spectra ($\lambda_{max,abs}$ and $\lambda_{max,em}$, Respectively), Molar Absorption Coefficients (ε), Emission Quantum Yields (ϕ), and Decay Times (τ)

compound	$\lambda_{max,abs}$ [nm, $\varepsilon \times 10^{-4}$ ($M^{-1}cm^{-1}$)]	$\lambda_{max,em}$ (nm)	ϕ (%)	τ (μs)
Re[T*p*CO_2CH_3PC](O)	441 (11.17), 555 (1.61), 587 (2.05)	776	1.2	66
Re[T*m*CO_2CH_3PC](O)	439 (8.37), 553 (1.20), 586 (1.57)	773	1.1	57
Pt[TPTBP]	430, 564, 614	770	21	47

https://dx.doi.org/10.1021/acsomega.0c01090
ACS Omega 2020, 5, 10596−10601

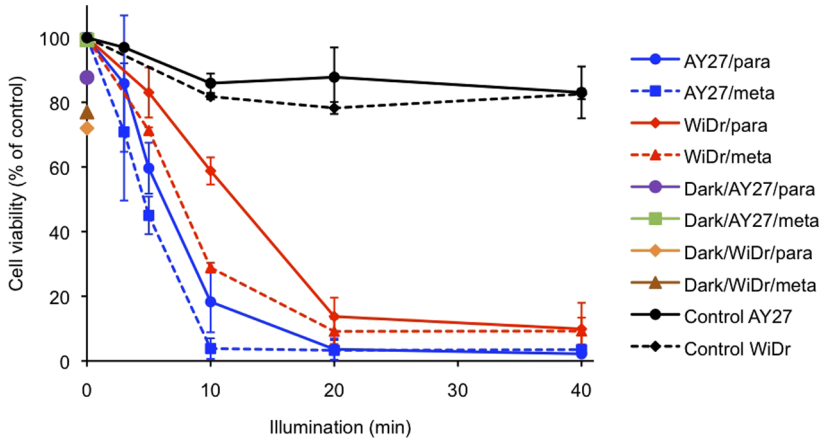

Figure 3. Viability of AY27 and WiDr cells upon incubation with Re[*m*TCPC](O) and Re[*p*TCPC](O) (10 μM, 24 h) as a function of blue light exposure (435 nm, 0−40 min). The black lines refer to control cells, which were exposed to light but not to a photosensitizer. Dark toxicity refers to the cell viability at 0 min of illumination on the *y* axis. Each data point is the average from three experiments ± SD relative to untreated cells.

under irradiation of solutions of sensitizers in ethanol with 595 ± 5 nm light, and the corresponding UV−vis spectra are summarized in Figure S11. The kinetics was virtually identical for the ester and carboxylic acid substituents and was also independent of the position of the substituent. It should be noted that the solutions contained 10% v/v of tetrahydrofuran (THF) to ensure solubility of the more lipophilic ester complexes. The Φ_Δ values obtained for all four corroles in EtOH/THF mixture are extremely similar (0.72 ± 0.02). We may conclude that all four compounds are powerful photosensitizers of singlet oxygen in spite of the very weak phosphorescence of the free acids.

PDT Experiments. The phototoxic/cytotoxic effects of the $Re^{V}O$ corrole free acids, Re[*m*TCPC](O) and Re[*p*TCPC](O), were evaluated for rat bladder cancer cells (AY27)[26,27] and human colon carcinoma cells (WiDr),[29] indicating that these compounds trigger cell changes leading to cell death (Figure 3). Cell viability was determined in both cell lines after incubation with the meta- and para-isomeric complexes (10 μM, 24 h). The concentration of the compounds was chosen on the basis of earlier PDT studies on AY27 cells with the analogous gold complexes (Au[*m*/*p*TCPC]) on the AY27 cell line with the analogous gold complexes (Au[*m*/*p*TCPC]) and the same light source.[14]

For both cell lines, the experiments described above showed a clear dependence of cell viability on the period of blue light exposure in the presence of the photosensitizer. For the AY27 cell line, both isomeric complexes were found to exhibit similar activity, resulting in 50% cell death after about 5 min of blue light exposure and essentially complete extermination after 10 min. For the WiDr cell line, the meta-isomer proved somewhat more active, effecting approximately 50% cell death in about 8 min of illumination and 95% in 20 min. During the same periods, the para-isomer achieved about 40 and 90% cell death. For comparison, illumination in the absence of a photosensitizer resulted in no more than 10% cell death after 40 min.

The effects of the photosensitizers on AY27 and WiDr cells were also investigated in the absence of light (dark toxicity). Incubation with the photosensitizers in the absence of light resulted in modest cell death rates for the WiDr cell line, about 23 and 28% after incubation (24 h, 37 °C) with the meta and para isomers of the photosensitizer, respectively (Figure 3, green and pink violet points, respectively). Much weaker dark toxicity was observed for the AY27 cells, with death rates around 1 and 12% after incubation with the meta and para isomers, respectively.

CONCLUSIONS

Along with our earlier work on gold corroles,[14] the present study underscores the growing importance of 5d metallocorroles as a new class of anticancer compounds, especially as photosensitizers in PDT. Within this family, the $Re^{V}O$ corroles have been of particular interest, by virtue of their ease of accessibility and superior thermal, chemical, and photochemical stability.[16] The new complexes reported here have delivered on that promise. The two esters studied, $Re^{V}O$ 5,10,15-tris(*meta*-carbomethoxyphenyl)corrole and $Re^{V}O$ 5,10,15-tris(*para*-carbomethoxyphenyl)corrole, exhibit phosphorescence quantum yields of approximately 1% and reasonably long phosphorescence lifetimes of about 60 μs in anoxic toluene. Much lower phosphorescence quantum yields on the order of 0.01% and somewhat shorter phosphorescent lifetimes were found for the $Re^{V}O$ carboxylic acids derived from the esters, probably because of efficient radiationless deactivation in aqueous/ethanolic media, in which these amphiphilic compounds were examined. The quantum yields for singlet oxygen formation, on the other hand, turned out to be equally high (0.72 ± 0.02) for both the esters and carboxylic acids. Gratifyingly, the $Re^{V}O$ carboxylic acids were found to exhibit high photocytotoxicity against rat bladder cancer cells (AY27) and human colon carcinoma cells (WiDr), achieving 50% cell death within 5−7 min of blue light exposure. Ongoing research in our laboratories accordingly focuses both on improved $Re^{V}O$ corrole-based phototherapeutics and on a wider evaluation of the expanding class of 5d metallocorroles.

EXPERIMENTAL SECTION

Chemical Syntheses and Characterization. *Materials and Instrumentation.* Except for solvents, all chemicals were obtained from Sigma-Aldrich and used as purchased. CHROMASOLV HPLC-grade *n*-hexane, dichloromethane, ethyl acetate, and toluene were used for column chromatography. Silica gel 60 (0.04−0.063 mm particle size; 230−400 mesh, Sigma) was used for column chromatography, and the columns used were generally about 12 cm in height and 3 cm

https://dx.doi.org/10.1021/acsomega.0c01090
ACS Omega 2020, 5, 10596−10601

in diameter. UV−vis spectra were recorded on an HP 8454 spectrophotometer at room temperature. High-resolution electrospray ionization (ESI) mass spectra were recorded on an LTQ Orbitrap XL spectrometer. ^{1}H NMR spectra were recorded on a Bruker Advance III HD 400 MHz spectrometer.

General Procedure for the Synthesis of Re^{V}O meso-(m/p-Carbomethoxyphenyl)corrole. To a 50 mL round-bottom flask equipped with a magnetic stirrer and reflux condenser, were added the free-base corrole H_3[T*p*/*m*CO_2CH_3PC] (100 mg, 0.142 mmol, 1 equiv), $Re_2(CO)_{10}$ (185 mg, 0.283 mmol, 2 equiv), potassium carbonate (100 mg), and 1,2,4-trichlorobenzene (8 mL). The contents were deoxygenated with argon and then heated to ∼180 °C overnight with constant stirring under argon. Upon cooling, the reaction mixture was loaded directly onto a silica gel column and chromatographed with *n*-hexane as the mobile phase, whereupon 1,2,4-trichlorobenzene eluted first. The desired complex eluted upon changing the eluent to dichloromethane and was further purified by preparative thin-layer chromatography with dichloromethane as the eluent.

Re[TpCO$_2$CH$_3$PC](O). Yield 68 mg (53.17%). UV−vis (CH_2Cl_2) λ_{max} [nm, $\varepsilon \times 10^{-4}$ (M^{-1} cm^{-1})]: 441 (11.17), 555 (1.61), 587 (2.05). ^{1}H NMR (400 MHz, −20 °C): δ 9.67 (d, 2H, $^3J_{HH}$ = 4.40 Hz, *β*-H); 9.32 (d, 4H, $^3J_{HH}$ = 4.48 Hz, *β*-H); 9.12 (d, 2H, $^3J_{HH}$ = 5.20 Hz, *β*-H); 8.66 (d, 2H, $^3J_{HH}$ = 7.52 Hz, 5,15-*o*1-Ph); 8.58 (d, 1H, $^3J_{HH}$ = 7.96 Hz, 10-*o*1-Ph); 8.52 (d, 2H, $^3J_{HH}$ = 8.20 Hz, 5,15-*o*2-Ph); 8.49 (d, 1H, $^3J_{HH}$ = 7.88 Hz, 10-*o*2-Ph); 8.41 (d, 2H, $^3J_{HH}$ = 7.84 Hz, 5,15-*m*2-Ph); 8.35 (d, 1H, $^3J_{HH}$ = 7.94 Hz, 10-*m*2-Ph); 8.16 (d, 2H, $^3J_{HH}$ = 7.60 Hz, 5,15-*m*1-Ph); 7.99 (d, 1H, $^3J_{HH}$ = 7.96 Hz, 10-*m*1-Ph); 4.03 (s, 6H, 5,15-*p*-CH_3); 4.01 (s, 3H, 10-*p*-CH_3). MS (ESI): M^+ 900.16 (expt), 900.15 (calcd for $C_{43}H_{29}N_4O_7Re$); elemental Anal. Calcd for $C_{43}H_{29}N_4O_7Re$: C, 57.39; H, 3.25; N, 6.23. Found: C, 57.89; H, 3.88; N, 5.78. IR ν_{ReO}: 989 cm^{-1}.

Re[TmCO$_2$CH$_3$PC](O). Yield 49 mg (39.27%). UV−vis (CH_2Cl_2) λ_{max} [nm, $\varepsilon \times 10^{-4}$ (M^{-1} cm^{-1})]: 439 (8.37), 553 (1.20), 586 (1.57). ^{1}H NMR (400 MHz, −20 °C): δ 9.72 (d, 2H, $^3J_{HH}$ = 4.04 Hz, *β*-H); 9.34 (d overlapping, 4H, $^3J_{HH}$ = 4.28 Hz, *β*-H); 9.25 (s, 1H, 5,15-*o*1m-Ph); 9.17 (s, 0.5H, 10-*o*1m-Ph); 9.13 (d, 2H, $^3J_{HH}$ = 4.68 Hz, *β*(−H); 8.82 (d, 1H, $^3J_{HH}$ = 7.60 Hz, 5,15-o1-Ph); 8.74 (1.5H, 5,15-o2m-Ph overlapping with 10-o1-Ph); 8.58 (s, 0.5H, 10-o2m-Ph); 8.48 (overlapping d, 3H, $^3J_{HH}$ = 6.88 Hz, 5,10,15-p-Ph); 8.32 (d, 1H, $^3J_{HH}$ = 7.20 Hz, 5,15-*o*2-Ph); 8.16 (d, 0.5H, $^3J_{HH}$ = 7.92 Hz, 10-*o*2-Ph); 8.04 (t, 1H, $^3J_{HH}$ = 7.72 Hz 5,15-*m*1-Ph); 7.99 (t, 0.5H, $^3J_{HH}$ = 7.56 Hz 10-*m*1-Ph); 7.92 (t, 1H, $^3J_{HH}$ = 8.00 Hz 5,15-*m*2-Ph); 7.86 (t, 0.5H, $^3J_{HH}$ = 7.72 Hz, 10-*m*2-Ph); 4.01 (s, 3H, 5,15-*m*1-CO_2CH_3); 3.98 (s, 1.5H, 10-*m*1-CO_2CH_3); 3.92 (s, 3H, 5,15-*m*2-CO_2CH_3); 3.88 (s, 1.5H, 10-*m*2-CO_2CH_3) note: The suffix m denotes the chemical shift in an atropisomeric species. MS (ESI): M^+ 900.16 (expt), 900.16 (calcd for $C_{43}H_{29}N_4O_7Re$); elemental Anal. Calcd for $C_{43}H_{29}N_4O_7Re$: C, 57.39; H, 3.25; N, 6.23. Found: C, 57.60; H, 3.12; N, 5.93. IR ν_{ReO}: 985 cm^{-1}.

Hydrolysis of Re^{V}O meso-(m/p-Carbomethoxyphenyl)-corrole. The Re^{V}O *meso*-(*m*/*p*-carbomethoxyphenyl)corrole (32 mg, 0.036 mmol) was dissolved in THF (50 mL) in a 250 mL round-bottom flask equipped with a magnetic stirrer and a reflux condenser. Aqueous NaOH (0.07 M, 20 mL) was added, and the mixture was heated at reflux (∼100 °C) for 24 h. Upon cooling to room temperature, the mixture was transferred to a separatory funnel containing ethyl acetate (150 mL) and washed with 0.5 M HCl. The organic phase was collected and washed three times with water, dried over anhydrous sodium sulfate, and filtered, and the filtrate was rotary evaporated to dryness. The residue was sonicated with a minimum volume of dichloromethane, and the resulting suspension was filtered. The residue on the filter paper was washed further with dichloromethane and collected as the pure Re[TCPC](O) product.

Re[pTCPC](O). Yield 19.7 mg (64.5%). UV−vis (THF) λ_{max} (nm), [$\varepsilon \times 10^{-4}$ (M^{-1} cm^{-1})]: 439 (11.06), 553 (1.34), 585 (1.87). MS (ESI): M^+ 858.11 (expt), 858.11 (calcd for $C_{40}H_{23}N_4O_7Re$); elemental Anal. Calcd for $C_{40}H_{23}N_4O_7Re\cdot H_2O$: C, 54.85; H, 2.88; N, 6.40. Found: C, 55.22; H, 3.25; N, 6.18. IR ν_{ReO}: 990 cm^{-1}.

Re[mTCPC](O). Yield 17.3 mg (56.6%). UV−vis (THF) λ_{max} (nm), [$\varepsilon \times 10^{-4}$ (M^{-1} cm^{-1})]: 438 (10.03), 553 (1.37), 586 (1.81). MS (ESI): M^+ 858.11 (expt), 857.10 (calcd for $C_{40}H_{23}N_4O_7Re$); elemental Analy. Calcd for $C_{40}H_{23}N_4O_7Re\cdot H_2O$: C, 54.85; H, 2.88; N, 6.40. Found: C, 54.44; H, 3.13; N, 6.23. IR ν_{ReO}: 992 cm^{-1}.

Photophysical Measurements. UV−vis absorption spectra were acquired on a Cary 50 UV−vis spectrophotometer (Varian), and emission spectra were acquired on a Fluorolog 3 fluorescence spectrometer (Horiba, Japan) equipped with NIR-sensitive photomultiplier R2658 (Hamamatsu, Japan). All spectra were corrected for the sensitivity of the photomultiplier. Relative luminescence quantum yields were determined, according to Crosby and Demas using the following equation:[34]

$$\phi_x = \phi_r \frac{S_x}{S_r} \frac{1 - 10^{-A_r}}{1 - 10^{-A_x}} \frac{{n_x}^2}{{n_r}^2}$$

where S_x and S_r are integrated areas under corrected emission spectra, A is the absorbance of the dye at the excitation wavelength, and n is the refractive index of the media, while x and r refer to analyzed dye and reference, respectively. Platinum(II) tetraphenyltetrabenzoporphyrin (Pt[TPTBP]) was used as the standard, for which a quantum yield of 21% had been determined in anoxic toluene.[30] Sample solutions in sealable quartz cells (Hellma Analytics, Mülheim, Germany) were deoxygenated by bubbling high purity nitrogen or argon (99.9999 and 99.999% purity, respectively, Linde gas, Austria) for at least 15 min. Luminescence decay times in solution were measured on the Fluorolog 3 spectrometer equipped with a DeltaHub module (Horiba) controlling a SpectraLED-456 lamp (λ = 456 nm) and using DAS-6 analysis software (Horiba) for data analysis.

Singlet oxygen quantum yields (Φ_Δ) were determined according to the literature procedure.[33] DMA was used as a singlet oxygen acceptor (c = 0.20 mM). A solution of DMA along with a sensitizer (concentration adjusted to identical absorbance at 595 nm) in EtOH/THF (9:1 v/v) was irradiated in a screw-cap quartz cuvette with the Xe lamp of the fluorometer (λ_{max} 595 nm, slit width 10 nm). Degradation of DMA was assessed via absorption measurements at 358 nm. The solution was magnetically stirred during irradiation and shaken after each irradiation period to ensure air-saturated conditions. Singlet oxygen quantum yields were determined relative to methylene blue, Φ_Δ = 0.48, which is the average of two values reported by Gross et al.[33] and Usui et al.[35]

PDT Experiments. *Materials and Instrumentation.* RPMI-1640 medium, L-glutamine, fetal bovine serum (FBS), sodium pyruvate, nonessential amino acids, trypsin, and

https://dx.doi.org/10.1021/acsomega.0c01090
ACS Omega 2020, 5, 10596−10601

phosphate buffered saline (PBS) were obtained from Gibco BRL, Life Technologies (Inchinnan, Scotland). Gentamicin sulfate was purchased from Schering Corp (Kenilworth, NJ), absolute ethanol from Arcus A/S (Oslo, Norway), and MTT [3-(4,5 dimethylthiazol-2-yl)-2,5-diphenyltetrazolium bromide] solution from Sigma-Aldrich (St. Louis, MO). Other chemicals were of the highest quality and commercially available.

The syngeneic rat bladder cancer cell line AY27 was kindly provided by Professor S. Selman, University of Ohio, USA, while the WiDr cell line was derived from a human primary adenocarcinoma of the rectosigmoid colon (P. Noguchi, 1979). Both cell lines were cultured in Corning/Sarstedt, 60 mm × 15 mm dishes, Nunc Denmark, and grown in RPMI-1640 medium, containing 10% v/v FBS, L-glutamine (80 mg/L), penicillin (100 U/mL), streptomycin (100 U/mL), and fungizone (0.25 mg/mL). The cell lines were grown in an atmosphere of 95% air and 5% CO_2 at 37 °C and were subcultured approximately twice a week.

In the phototoxicity measurements, cells at room temperature were illuminated from below by a LumiSource (PCI Biotech AS, Oslo) lamp. The lamp is designed to provide homogenous illumination of living cells in an in vitro setting across an area of 45 × 17 cm. The lamp consists of four tubes (4 × 18 W Osram L 18/67) that emit light at a peak wavelength of 435 nm, resulting in 13 mW/cm^2 light intensity at the cells, that is, near the bottom of cell dishes. Both light-sensitive solutions and cells were covered with aluminum foil during the entire experiments. All dishes were covered with aluminium foil and incubated for 24 h (37 °C, 5% CO_2).

Viability Assays on AY27 and WiDr Cancer Cell Lines. Day 1. The cells were washed with PBS, harvested from the cultivation flasks, and loosened with trypsin (2%, 3 mL). After 3−5 min, growth medium (10 mL) was added, and the cell suspension was transferred to a 50-mL tube and centrifuged (5 min, 1500 rpm, 4 °C), followed by removal of dead cells. The cell pellet was carefully resuspended in the growth medium (0.5 mL), prior to further dilution with growth medium to a total volume of 10 mL. The cell suspension (20 μL) was then added to a Bürker chamber. The cell numbers in four 1 mm^2 squares were manually counted, which provided the cell concentration in the stock solution. After dilution with growth medium, the cells were seeded in 6 cm Petri dishes containing 3 mL of cell suspension (0.25−0.35 × 10^6 cells/dish). The dishes were incubated for ∼24 h at 37 °C, with each experiment including 20−30 dishes.

Day 2. Growth medium was removed, and new medium was added (3 mL, 37 °C) to the control dishes (without the photosensitizer). For PDT experiments, growth medium was removed, and photosensitizer-containing medium (10 μM, 3 mL, 37 °C) was added to the remaining dishes in the dark. Cells with only photosensitizer-containing medium were used for dark toxicity assessments while samples without any treatment (with either light or photosensitizer) were used as controls. After a postincubation period (24 h, 37 °C, 5% CO_2) after illumination, the MTT cell proliferation assay[36,37] was performed as follows: Growth medium was removed, and the cells were incubated in MTT solution (0.5 mg/mL, 1 h, 37 °C, 5% CO_2, Sigma-Aldrich, St. Louis, MO). The MTT solution was then decanted off and replaced by isopropanol (2 mL). The dishes were then placed on a plate shaker for (200 rpm) 30 min. Dead cells were then removed by centrifuging the cell suspensions (5 min, 1500 rpm), as previously described for the AY27 cell line.[26] The absorbance of the supernatant was measured at 595 nm with a Shimadzu UV-1700 spectrophotometer. The data so obtained were processed and compared with those for cells without any treatment (with either light or photosensitizer).

Day 3. The control dishes (which did not undergo either light nor photosensitizer) were washed twice with PBS (3 mL, 37 °C), followed by addition of growth medium (3 mL, 37 °C), and placed in an incubator (37 °C, 5% CO_2). Additional PBS was added (3 mL, 37 °C) to all the other dishes before illumination with blue light. After illumination over different time intervals, the PBS was removed, and growth medium was added (3 mL, 37 °C). All dishes were then placed under further incubation (24 h, 37 °C).

Day 4. Twenty-four hours after illumination, MTT assays were performed to measure the indirect activity of living cells. MTT working solutions (0.5 mg/mL) were freshly made using a 1:9 mixture of MTT stock solution (5 mg/mL, 37 °C) and growth medium (37 °C). All the dishes were carefully washed with PBS (2 mL) before the MTT working solution (2 mL, 1 h, 37 °C) was added. After incubation, the MTT working solution was removed, and isopropanol (2 mL, room temperature) was added before the Petri dishes were placed on an orbital shaker (30 min, 70 rpm). The shaken suspensions were transferred to 15 mL tubes and centrifuged (5 min, 1500 rpm, 4 °C). The supernatants were transferred into cuvettes and diluted 10-fold with isopropanol. The absorbance at λ_{ex} = 595 nm was measured on a double-beam UV−vis spectrophotometer (UV-1700 Shimadzu, Japan) using isopropanol as reference.

■ ASSOCIATED CONTENT

Supporting Information

The Supporting Information is available free of charge at https://pubs.acs.org/doi/10.1021/acsomega.0c01090.

UV−vis spectra, phosphorescence decays, NMR, mass, and IR spectra (PDF)

■ AUTHOR INFORMATION

Corresponding Authors

Sergey M. Borisov − *Institute of Analytical Chemistry and Food Chemistry, Graz University of Technology, 8010 Graz, Austria;* orcid.org/0000-0001-9318-8273; Email: sergey.borisov@tugraz.at

Abhik Ghosh − *Department of Chemistry, UiT—The Arctic University of Norway, N-9037 Tromsø, Norway;* orcid.org/0000-0003-1161-6364; Email: abhik.ghosh@uit.no

Odrun A. Gederaas − *Department of Clinical and Molecular Medicine and Department of Physics, Norwegian University of Science and Technology, NTNU, N-7491 Trondheim, Norway;* Email: odrun.gederaas@ntnu.no

Authors

Rune F. Einrem − *Department of Chemistry, UiT—The Arctic University of Norway, N-9037 Tromsø, Norway*

Abraham B. Alemayehu − *Department of Chemistry, UiT—The Arctic University of Norway, N-9037 Tromsø, Norway;* orcid.org/0000-0003-0166-8937

Complete contact information is available at: https://pubs.acs.org/10.1021/acsomega.0c01090

https://dx.doi.org/10.1021/acsomega.0c01090
ACS Omega 2020, 5, 10596−10601

Notes

The authors declare no competing financial interest.

■ ACKNOWLEDGMENTS

This work was supported by the Research Council of Norway (grant no. 262229 to A.G.), with supplementary funding from the Cancer Research Foundation of St. Olav's University Hospital, Trondheim. We thank Matthias Schwar (TU Graz) for the singlet oxygen assays.

■ REFERENCES

(1) Bonnett, R. *Chemical Aspects of Photodynamic Therapy*; CRC: Boca Raton, FL, 2000; p 324.
(2) *Handbook of photodynamic therapy : updates on recent applications of porphyrin-based compounds*; Pandey, R. K., Kessel, D., Dougherty, T. J., Eds.; World Scientific: New Jersey, 2016; p 564.
(3) Patrice, T.; Moan, J.; Peng, Q. An outline of the history of PDT. *Photodynamic Therapy*; Royal Society of Chemistry: London, 2003, pp 1−18.
(4) Spikes, J. D. Porphyrins and related compounds as photodynamic sensitizers. *Ann. N.Y. Acad. Sci.* **1975**, *244*, 496−508.
(5) Bonnett, R. Photosensitizers of the porphyrin and phthalocyanine series for photodynamic therapy. *Chem. Soc. Rev.* **1995**, *24*, 19−33.
(6) Sternberg, E. D.; Dolphin, D.; Brückner, C. Porphyrin-based photosensitizers for use in photodynamic therapy. *Tetrahedron* **1998**, *54*, 4151−4202.
(7) Abrahamse, H.; Hamblin, M. R. New photosensitizers for photodynamic therapy. *Biochem. J.* **2016**, *473*, 347−364.
(8) Ethirajan, M.; Chen, Y.; Joshi, P.; Pandey, R. K. The Role of Porphyrin Chemistry in Tumor Imaging and Photodynamic Therapy. *Chem. Soc. Rev.* **2011**, *40*, 340−362.
(9) Ghosh, A. Electronic Structure of Corrole Derivatives: Insights from Molecular Structures, Spectroscopy, Electrochemistry, and Quantum Chemical Calculations. *Chem. Rev.* **2017**, *117*, 3798−3881.
(10) Nardis, S.; Mandoj, F.; Stefanelli, M.; Paolesse, R. Metal complexes of corrole. *Coord. Chem. Rev.* **2019**, *388*, 360−405.
(11) Teo, R. D.; Hwang, J. Y.; Termini, J.; Gross, Z.; Gray, H. B. Fighting Cancer with Corroles. *Chem. Rev.* **2017**, *117*, 2711−2729.
(12) Jiang, X.; Liu, R. X.; Liu, H. Y.; Chang, C. K. Corrole-based photodynamic antitumor therapy. *J. Chin. Chem. Soc.* **2019**, *66*, 1090−1099.
(13) Teo, R. D.; Gray, H. B.; Lim, P.; Termini, J.; Domeshek, E.; Gross, Z. A Cytotoxic and Cytostatic Gold(III) Corrole. *Chem. Commun.* **2014**, *50*, 13789−13792.
(14) Alemayehu, A. B.; Day, N. U.; Mani, T.; Rudine, A. B.; Thomas, K. E.; Gederaas, O. A.; Vinogradov, S. A.; Wamser, C. C.; Ghosh, A. Gold Tris(carboxyphenyl)corroles as Multifunctional Materials: Room Temperature Near-IR Phosphorescence and Applications to Photodynamic Therapy and Dye-Sensitized Solar Cells. *ACS Appl. Mater. Interfaces* **2016**, *8*, 18935−18942.
(15) Lemon, C. M.; Powers, D. C.; Brothers, J.; Nocera, D. G. Gold Corroles as Near-IR Phosphors for Oxygen Sensing. *Inorg. Chem.* **2017**, *56*, 10991−10997.
(16) Einrem, R. F.; Gagnon, K. J.; Alemayehu, A. B.; Ghosh, A. Metal-Ligand Misfits: Facile Access to Rhenium-Oxo Corroles by Oxidative Metalation. *Chem.—Eur. J.* **2016**, *22*, 517−520.
(17) Alemayehu, A. B.; Teat, S. J.; Borisov, S. M.; Ghosh, A. Rhenium-Imido Corroles. *Inorg. Chem.* **2020**, *59*, 6382−6389.
(18) Alemayehu, A. B.; Gagnon, K. J.; Terner, J.; Ghosh, A. Oxidative Metalation as a Route to Size-Mismatched Macrocyclic Complexes: Osmium Corroles. *Angew. Chem., Int. Ed.* **2014**, *53*, 14411−14414.
(19) Palmer, J. H.; Day, M. W.; Wilson, A. D.; Henling, L. M.; Gross, Z.; Gray, H. B. Iridium Corroles. *J. Am. Chem. Soc.* **2008**, *130*, 7786−7787.
(20) Alemayehu, A. B.; Vazquez-Lima, H.; Beavers, C. M.; Gagnon, K. J.; Bendix, J.; Ghosh, A. Platinum corroles. *Chem. Commun.* **2014**, *50*, 11093−11096.
(21) Borisov, S. M.; Einrem, R. F.; Alemayehu, A. B.; Ghosh, A. Ambient-temperature near-IR phosphorescence and potential applications of rhenium-oxo corroles. *Photochem. Photobiol. Sci.* **2019**, *18*, 1166−1170.
(22) Borisov, S. M.; Alemayehu, A.; Ghosh, A. Osmium-Nitrido Corroles as NIR Indicators for Oxygen Sensors and Triplet Sensitizers for Organic Upconversion and Singlet Oxygen Generation. *J. Mater. Chem. C* **2016**, *4*, 5822−5828.
(23) Palmer, J. H.; Durrell, A. C.; Gross, Z.; Winkler, J. R.; Gray, H. B. Near-IR Phosphorescence of Iridium(III) Corroles at Ambient Temperature. *J. Am. Chem. Soc.* **2010**, *132*, 9230−9231.
(24) Sinha, W.; Ravotto, L.; Ceroni, P.; Kar, S. NIR-Emissive Iridium(III) Corrole Complexes as Efficient Singlet Oxygen Sensitizers. *Dalton Trans.* **2015**, *44*, 17767−17773.
(25) Alemayehu, A. B.; MCormick, L. J.; Gagnon, K. J.; Borisov, S. M.; Ghosh, A. Stable Platinum(IV) Corroles: Synthesis, Molecular Structure, and Room-Temperature Near-IR Phosphorescence. *ACS Omega* **2018**, *3*, 9360−9368.
(26) Gederaas, O. A.; Johnsson, A.; Berg, K.; Manandhar, R.; Shrestha, C.; Skåre, D.; Ekroll, I. K.; Høgset, A.; Hjelde, A. Photochemical internalization in bladder cancer - development of an orthotopic in vivo model. *J. Photochem. Photobiol. Sci.* **2017**, *16*, 1664−1676.
(27) Larsen, E. L.; Randeberg, L. L.; Gederaas, O. A.; Arum, C. J.; Hjelde, A.; Zhao, C. M.; Chen, D.; Krokan, H. E.; Svaasand, L. O. Monitoring of hexyl 5-aminolevulinate-induced photodynamic therapy in rat bladder cancer by optical spectroscopy. *J. Biomed. Opt.* **2008**, *13*, 044031.
(28) Lindgren, M.; Gederaas, O. A.; Siksjø, M.; Hansen, T. A.; Chen, L.; Mettra, B.; Andraud, C.; Monnereau, C. Influence of Polymer Charge on the Localization and Dark- and Photo-Induced Toxicity of a Potential Type I Photosensitizer in Cancer Cell Models. *Molecules* **2020**, *25*, 1127.
(29) Noguchi, P.; Wallace, R.; Johnson, J.; Earley, E. M.; O'Brien, S.; Ferrone, S.; Pellegrino, M. A.; Milstien, J.; Needy, C.; Browne, W.; Petricciani, J. Characterization of WiDr: A human colon carcinoma cell line. *In Vitro* **1979**, *15*, 401−408.
(30) Zach, P. W.; Freunberger, S. A.; Klimant, I.; Borisov, S. M. Electron-Deficient Near-Infrared Pt(II) and Pd(II) Benzoporphyrins with Dual Phosphorescence and Unusually Efficient Thermally Activated Delayed Fluorescence: First Demonstration of Simultaneous Oxygen and Temperature Sensing with a Single Emitter. *ACS Appl. Mater. Interfaces* **2017**, *9*, 38008−38023.
(31) *Hydrogen Bonding and Transfer in the Excited State, I & II*; Han, K.-L., Zhao, G.-J., Eds.; Wiley: Hoboken, NJ, 2011.
(32) *Fluorescence Spectroscopy in Biology: Advanced Methods and their Applications to Membranes, Proteins, DNA, and Cells*; Hof, M., Hutterer, R., Fidler, V., Eds.; Springer: Heidelberg, 2005.
(33) Gross, E.; Ehrenberg, B.; Johnson, F. M. Singlet Oxygen Generation by Porphyrins and the Kinetics of 9,10-Dimethylanthracene Photosensitization in Liposomes. *Photochem. Photobiol.* **1993**, *57*, 808−813.
(34) Crosby, G. A.; Demas, J. N. Measurement of photoluminescence quantum yields. Review. *J. Phys. Chem.* **1971**, *75*, 991−1024.
(35) Usui, Y.; Koike, H.; Kurimura, Y. An Efficient Regeneration of Singlet Oxygen from 2,5-Diphenylfuran Endoperoxide Produced by a Dye-Sensitized Oxygenation. *Bull. Chem. Soc. Jpn.* **1987**, *60*, 3373−3378.
(36) Mosmann, T. Rapid Colorimetric Assay for Cellular Growth and Survival: Application to Proliferation and Cytotoxicity Assays. *J. Immunol. Methods* **1983**, *65*, 55−63.
(37) Carmichael, J.; DeGraff, W. G.; Gazdar, A. F.; Minna, J. D.; Mitchell, J. B. Evaluation of a tetrazolium-based semiautomated colorimetric assay: assessment of radiosensitivity. *Cancer Res.* **1987**, *47*, 943−946.

https://dx.doi.org/10.1021/acsomega.0c01090
ACS Omega 2020, 5, 10596−10601